Ice particles sink below the water surface due to a balance of salt, van der Waals and buoyancy forces

Priyadarshini Thiyam[a,b,c], Johannes Fiedler[b,d], Stefan Y. Buhmann[d], Clas Persson[a,b], Iver H. Brevik[c], Mathias Boström[c], and Drew F. Parsons[e,1]

[a]Department of Materials Science and Engineering, KTH Royal Institute of Technology, SE-100 44 Stockholm, Sweden; [b]Centre for Materials Science and Nanotechnology, Department of Physics, University of Oslo, P.O. Box 1048 Blindern, NO-0316 Oslo, Norway; [c]Department of Energy and Process Engineering, Norwegian University of Science and Technology, NO-7491 Trondheim, Norway; [d]Physikalisches Institut, Albert-Ludwigs-Universität Freiburg, Hermann-Herder-Str. 3, 79104 Freiburg, Germany; [e]School of Engineering and IT, Murdoch University, 90 South St, Murdoch, WA 6150, Australia

This manuscript was compiled on February 28, 2018

According to the classical Archimedes' principle ice floats in water and has a fraction of its volume above the water surface. However, for very small ice particles, other competing forces such as van der Waals forces due to fluctuating charge distributions and ionic forces due to salt ions and charge on the ice surface also contribute to the force balance. The latter crucially depend on both the pH of the water and the salt concentration. The role of these forces in governing the initial stages of ice condensation has never been considered. Here we show that small ice particles can only form below an exclusion zone, from 2 nm (in high salt concentrations) up to 1 μm (in pure water at pH 7) thick, under the water surface. This distance is defined by an equilibrium of upwards buoyancy forces and repulsive van der Waals forces. Ionic forces due to salt and ice surface charge push this zone further down. Only after growing to a radius larger than 10 μm will the ice particles eventually float towards the water surface in agreement with the simple intuition based on Archimedes' principle. Our result is the first prediction of observable repulsive van der Waals forces between ice particles and the water surface outside a laboratory setting. We posit that it has consequences on the biology of ice water as we predict an exclusion zone free of ice particles near the water surface which is sufficient to support the presence of bacteria.

ice submersion | exclusion zone | van der Waals | salt effect | ice charge

1. Introduction

It is well known that ice growth usually starts on a water surface due to differences in density of water and ice. In this paper we present calculations that suggest, however, that the initial ice formation in ice cold water does not always occur at the water-air surface but as an aggregation of small clusters at some distance below. It has been discussed in the literature that the so-called frazil ice can form as thin structures of ice mixed among the ocean surface layers by turbulent fluid motion as long as the buoyancy force is not large enough to lift them to the surface (1, 2). For small clusters, we find a stable equilibrium separation from the water surface, where the repulsive van der Waals forces and the buoyancy force due to gravity balance each other. As the cluster grows, the buoyancy force scales stronger with the cluster size than the Lifshitz force and the clusters start rising towards the surface. Eventually, the cluster starts to float on the water, but with repulsive Lifshitz forces establishing a thin layer of water at the ice-air interface, as studied previously (3–9).

We present calculations describing explicitly how the dispersion interaction of small ice clusters of the order of few nanometers in radius, and larger ice particles (modeled here as spheres) in water at temperature $T = 273.16$ K exhibits repulsive-attractive force transitions near a water surface. The dispersion (i. e., Casimir-Polder, van der Waals or Lifshitz) force combined with buoyancy force drives the ice cluster close to the water surface. Planes of ice spheres are involved at an initial stage in ice formation near a water surface. Our simplified model systems are shown in Fig. 1. Comparing the sphere radius to the separation of the sphere from the water-air interface, we consider the two extremes of small spheres (Casimir-Polder interaction) and large spheres (Lifshitz interaction). The former drives the ice cluster (together with buoyancy force) towards the water surface. For the latter case, given the short distances between the the ice sphere and the water surface compared to the sphere size, it is realistic to use the Derjaguin approximation combined with the Lifshitz interaction. Based on analysis of the separations where repulsion is observed, the model in subfigure (ii) of Fig. 1 is more appropriate for ice clusters considered to be substantially larger than 100 nm. The resulting Lifshitz force is compared with the net buoyancy force, and we give estimates for the maximum ice sphere size for which repulsive Lifshitz force overcomes the gravitational buoyancy force. In order to make firm predictions we need to extend the theory to account for

Significance Statement

We present a model of ice-water-air interactions which demonstrate that microscopic ice particles submerge below the air-water interface. Repulsive van der Waals interactions and salt effects associated with charge on the ice surface are sufficiently strong to overcome buoyancy when the particle is smaller than 10 μ in radius. This results in an exclusion zone free of microscopic ice, as large as 1 micron deep depending on salt concentration. We suggest this exclusion zone may be exploited by microbes to stabilise attachment on macroscopic ice bodies.

MB and PT initiated the project. PT performed Lifshitz energy and Casimir-Polder energy calculations. JF and SYB contributed the finite size extension to the Casimir-Polder energy. SYB provided the analytical estimate of the equilibrium position. CP supervised PT, administered Norwegian projects, and discussed results and implications. IB contributed to the general theory. DFP calculated and analysed Salt and Charge Effects and prepared the discussion on Consequences for Life. All contributed equally to the writing of the manuscript and took part in analysis and discussion of the results.

The authors declare no conflict of interest.

[1]To whom correspondence should be addressed. E-mail: D.Parsons@murdoch.edu.au

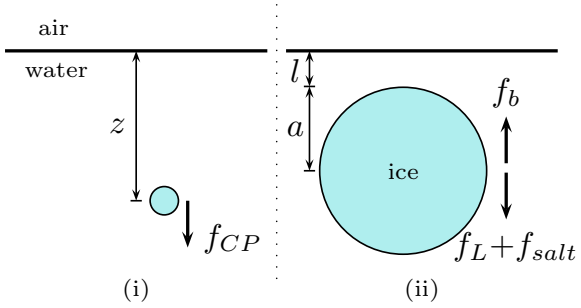

Fig. 1. (Color online) Schematic figures for our model system. Subfigure (i) shows a small ice particle a distance z from a water-air surface. Subfigure (ii) displays a large ice sphere close to a water-air surface; this system being used to calculate the Lifshitz force with the Derjaguin approximation. (Based on analysis of the separations where repulsion is observed, the model depicted in subfigure (ii) is more appropriate for ice clusters substantially larger than 3 nm).

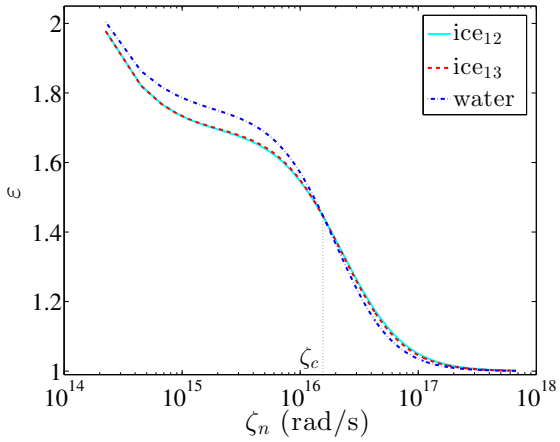

Fig. 2. (Color online) Two models of dielectric function of ice described by Elbaum and Schick. The blue curve shows the permittivity as function of frequency for water. The static values, $\varepsilon(0)$, for ice and water are 91.5 and 88.2, respectively, using data from Elbaum and Schick (3). The data points for different Matsubara frequencies (ζ_n) are joined by lines.

the presence of surface charges. We demonstrate that double layer forces push the tiny ice clusters further from the surface. Once the ice clusters reach a size of around few hundred micrometers, it will become dominated by buoyancy force and show the expected behaviour described by the Archimedes principle. We start with a description of the theory used to calculate buoyancy, van der Waals and double layer forces. We then discuss how these forces combine to stabilize tiny ice clusters below the water-air interface.

2. Theory

In order to evaluate the forces on an ice particle near the air-water interface, we follow the philosophy of the theory of colloidal stability developed by Derjaguin and Landau (10), and Verwey and Overbeek (DLVO theory) (11). This theory separates the Lifshitz (van der Waals) force f_L acting on the ice particle from salt forces f_{salt} (electrostatic and entropic) arising from adsorption of ions and associated effects on the charge of the ice surface. Alongside these conventional DLVO forces we add the buoyancy force f_b due to gravity, so the total force acting on the ice particle is

$$f_{tot}(l) = f_b(l) + f_L(l) + f_{\mathrm{salt}}(l), \qquad [1]$$

where l is the distance between the ice surface and the air-water interface; see Fig. 1. In this manuscript we evaluate the equilibrium distance l_{eq}, where the forces are in balance, stabilizing the position of the particle with $f_{tot}(l_{eq}) = 0$.

A. Buoyancy force. Since ice is less dense than water, the buoyancy force f_b is attractive, pushing the ice particle in water towards the water-air interface. While the particle is fully submersed in water, the buoyancy force is independent of l, with

$$f_b = \frac{4\pi a^3}{3} g(\rho_{\mathrm{ice}} - \rho_{\mathrm{water}}), \qquad [2]$$

where a is the spherical radius of the ice particle. $\rho_{\mathrm{ice}} = 9.167 \times 10^3\ \mathrm{kg\,m^{-3}}$ and $\rho_{\mathrm{water}} = 9.998 \times 10^3\ \mathrm{kg\,m^{-3}}$ are the mass densities of ice and water, respectively (12), and g is the gravitational constant $9.8\ \mathrm{m\,s^{-2}}$. The buoyancy force could be extended further to include the case of $l < 0$ for large ice particles, where the top of the ice particle rises above the air-water interface (the iceberg effect), which may also involve curvature of the air-water interface at the 3-phase contact point (13, 14). However we are interested in the case of microparticles with $l > 0$, for which the constant buoyancy force of Eq. 2 applies. The attractive buoyancy force, normalised by particle size (vis–à–vis a^3) therefore assumes a constant value of $f_b/a^3 \approx -3.41 \times 10^3\ \mathrm{N\,m^{-3}}$.

B. van der Waals Interaction. We represent the van der Waals interaction on the ice particle using the retarded Lifshitz force acting on a large ice sphere near a water surface (when $a \gg l = z - a$ where l is the distance between sphere surface and water surface; see right subfigure in Fig. 1) as given from the Derjaguin approximation. The force is then $f_L(l) = 2\pi a F(l)$, where F is the Lifshitz free energy per unit area between parallel surfaces a distance l apart (15, 16)

$$f_L(l) = k_B T a \sum_{n=0}^{\infty}{}' \left(g^s + g^p\right), \qquad [3]$$

where k_B is the Boltzmann constant and T the temperature. The prime indicates that the $n = 0$ term carries a weight 1/2. The spectral functions for s-polarized (transverse electric) and p-polarized (transverse magnetic) modes g^X $(X = s, p)$ are

$$g^X(i\zeta_n) = \int_0^\infty q\, dq \ln[1 - r_{21}^{\mathrm{X}} r_{23}^{\mathrm{X}} e^{-2\gamma_2 l}]. \qquad [4]$$

The reflection coefficients are given by

$$r_{ij}^p = \frac{\varepsilon_j\gamma_i - \varepsilon_i\gamma_j}{\varepsilon_j\gamma_i + \varepsilon_i\gamma_j}, \quad \text{and} \quad r_{ij}^s = \frac{\gamma_i - \gamma_j}{\gamma_i + \gamma_j}, \qquad [5]$$

and the transversal part of the wave vector in the i-th layer $\gamma_i(i\zeta_n) = \sqrt{q^2 + (\zeta_n/c)^2\varepsilon_i}$. To model dispersion forces acting on an ice cluster near a water-air interface we acquire the dielectric functions for ice, $\varepsilon_{ice}^{12/13}$, and for water, ε_{water}, at $T = 273.16\,\mathrm{K}$ from Elbaum and Schick (3). These are plotted in Fig. 2.

The Lifshitz interaction, modulated for a curved particle using the proximity force (Derjaguin) approximation, is appropriate for conditions where the distance l between the ice particle and the water-air interface is small relative to the radius a of the ice particle. At longer distances, the Casimir-Polder representation of the van der Waals force (17–19) could be employed. But we find this long range Casimir-Polder force to be weak relative to buoyancy (see Supporting Information). A particle far from the air-water interface will move upwards under buoyancy, until it reaches distances at which the Lifshitz (or salt) force starts to dominate over buoyancy.

C. Salt and Charge Effects. Alongside buoyancy and the van der Waals interaction, an interaction between the ice particle and the water-air interface arises due to charge on the ice surface and consequent physisorption of salt ions. This force is repulsive, driving the ice microparticle further away from the air-water interface. The surface charge of ice can be described with an amphoteric charge regulation model (20). Dissociation of water molecules on the ice surface liberates H^+, forming a negative surface charge, while chemisorption of H^+ forms a positive charge. We use parameters suggested by Kallay *et al.*, with site density $10^{-5}\,\mathrm{mol\,m^{-2}}$ and dissociation constants

$$-\mathrm{OH} \rightleftharpoons -\mathrm{O}^- + \mathrm{H}^+ \quad (\mathrm{p}K_- = +5.8), \qquad [6]$$

$$\mathrm{OH_2}^+ \rightleftharpoons -\mathrm{OH} + \mathrm{H}^+ \quad (\mathrm{p}K_+ = +1.0). \qquad [7]$$

These parameters provide an isoelectric point of 3.5. We also apply Kallay's description of the chemisorption of salt anions:

$$-\mathrm{ONa} \rightleftharpoons -\mathrm{O}^- + \mathrm{Na}^+ \quad (\mathrm{p}K_{\mathrm{Na}} = +5.2), \qquad [8]$$

$$-\mathrm{OH\cdot NO_3}^- \rightleftharpoons -\mathrm{OH} + \mathrm{NO_3}^- \quad (\mathrm{p}K_{\mathrm{NO_3}} = +3.1). \qquad [9]$$

We use Parsons and Salis' theory to describe the surface charge and chemisorption free energy under competitive binding conditions (including double binding of H^+ and NO_3^-) (21). Here we use only the electrostatic potential to determine ion concentration profiles, i.e. we neglect nonelectrostatic interactions such as ion dispersion (these are important for describing specific ion effects, but not for the broad ice-water interactions studied here). We determine the electrostatic potential and ion profiles using the Poisson-Boltzmann model, implemented using finite element methods (22). That is, ion concentration profiles are determined from the electrostatic Boltzmann distribution, $c_i(z) = c_{i0}\exp(-q_i\psi(z)/kT)$, where c_{i0} is the bulk concentration of ion i. The electrostatic potential is obtained by solving Poisson's equation, $\nabla\varepsilon_{vac}\varepsilon_0\nabla\psi = -\sum_i q_i c_i(z)$. The calculated surface potential and surface charge of ice in various salt concentrations and pH are provided in Supplementary Information.

The electric field and ion concentration profiles provide contributions to the interaction force between the ice particle and the water-air interface (applying the Derjaguin approximation)

$$f_{\mathrm{salt}}(l) = 2\pi a(F_{el} + F_{en}), \qquad [10]$$

where F_{el} refers to the electrostatic surface free energy of a flat ice surface,

$$F_{el} = \frac{1}{2}\int_0^l dz\varepsilon_{vac}\varepsilon_0 E^2, \qquad [11]$$

with $E = -\nabla\psi$, and F_{en} is the entropic configuration energy

$$F_{\mathrm{en}} = kT\sum_i \int_0^l dz\left\{c_i(z)\ln\frac{c_i(z)}{c_{i0}} - c_i(z) + c_{i0}\right\}. \qquad [12]$$

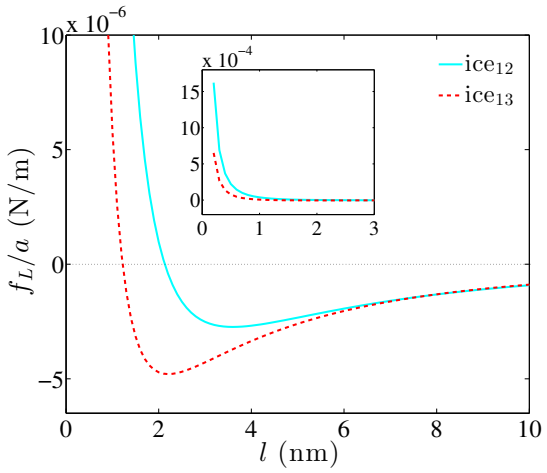

Fig. 3. (Color online) The normalised Lifshitz force (f_L/a) versus l for both ice models. The inset shows it on an expanded scale.

3. Results and discussion

We first discuss the balance of van der Waals and buoyancy forces alone and the resulting equilibrium distances owing to this balance for spheres of growing size a. We then proceed to study the same with the inclusion of salt effects.

A. Balance of van der Waals and buoyancy forces. We consider how the van der Waals force alone balances against buoyancy, taking a system of pure ideal water represented by its dielectric spectrum alone, with no ions in solution and no charge on the ice surface. Physically this corresponds to the system at the isoelectric point, or to highly saline water where charges are screened. The Lifshitz force under the Derjaguin approximation scales with the first power of the sphere radius a, displayed in Fig. 3 (we note that the Casimir–Polder force application to very long distances scales to the third power of radius, and is inadequate to balance the buoyant force which scales the same; see Supporting Information). We find a repulsive dispersion force at small distances. The repulsive to attractive force transition can be roughly estimated to take place at $l_{transition} \approx c/(2\zeta_c\sqrt{\varepsilon_{water}(\zeta_c)})$, where ζ_c is the frequency at which ice and water dielectric functions cross. Here, $\zeta_c \approx 1.6\times10^{16}\,\mathrm{rad\,s^{-1}}$ and $\varepsilon_{water}(\zeta_c) \approx 1.5$ which gives $l_{transition}$ to be approximately 7.7 nm. In practice one needs to perform the calculations in detail to get the actual equilibrium distance, since it depends on sensitive cancellations between positive and negative contributions.

The balance of the dispersion force against the buoyancy force, where $f_b + f_L(l_{eq}) = 0$, results in a size-dependent equilibrium distance l_{eq}, displayed in Fig. 4. For all predicted values of sphere size and corresponding equilibrium distance, the distance is orders of magnitude below the radius, so that our description with the Derjaguin approximation is well satisfied. We observe that with increasing size of the ice sphere the layer of water between ice and air decreases. Eventually, the ice structures are so big that they reach the water surface due to the buoyancy force which of course is in line with the classical Archimedes' principle. The final stages of sphere growth and corresponding approach to the water-air interface can be understood from a simple analytical model.

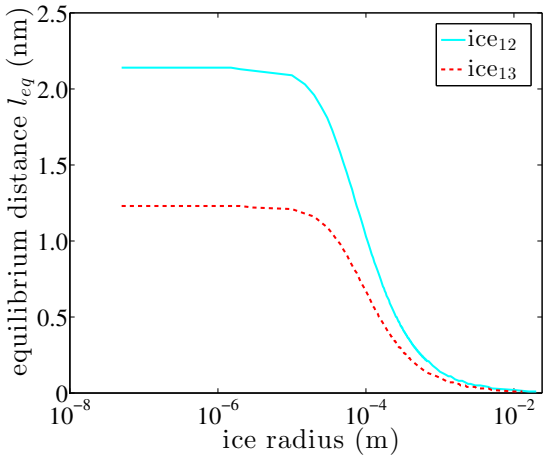

Fig. 4. (Color online) Equilibrium distance l_{eq} as a function of the sphere radii for both ice models. This is obtained as the distance with zero total force when adding net buoyancy force and Lifshitz force (i.e. when $f_b + f_L(l_{eq}) = 0$).

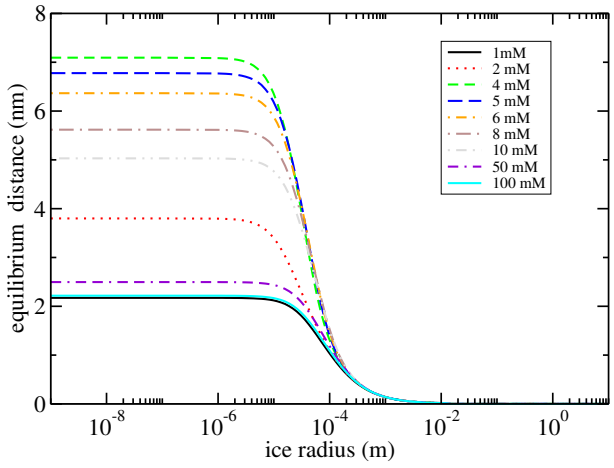

Fig. 5. (Color online) Equilibrium distance l_{eq} as a function of the sphere radii with the ice surface charged at the isoelectric point (pH 3.5). This is obtained as the distance with zero total force when adding net buoyancy force, Lifshitz force and forces due to salt ions (i.e. when $f_b + f_L(l_{eq}) + f_{\rm salt}(l_{eq}) = 0$). Curves are shown for a range of background $NaNO_3$ salt concentrations.

At very small distances, the Lifshitz–Derjaguin force can be approximated by its nonretarded limit $f_L(l) = Ca/l^2$ where the constant reads $C = 6.8 \times 10^{-23}$ N m for ε^{12}_{ice} dielectric function of ice and $C = 3.0 \times 10^{-23}$ N m for ε^{13}_{ice}. Recalling that $f_b = -Da^3$ with $D \approx 3.41 \times 10^3$ N m^{-3}, the equilibrium condition $f_b + f_L(l_{eq}) = 0$ then reads

$$Da^3 = \frac{Ca}{l^2}, \qquad [13]$$

so that

$$l_{eq} = \sqrt{\frac{C}{D}}\,\frac{1}{a}\,. \qquad [14]$$

It follows that experimental measurement of the equilibrium distance for ice particles of different radii could be used to determine the van der Waals coefficient C.

B. Balance of salt, van der Waals and buoyancy forces. The addition of salt introduces two significant variables: the pH of the aqueous solution, and the concentration of salt. The pH controls the ice surface charge. The case considered above, balancing van der Waals forces only against buoyancy, roughly corresponds to behaviour at the isoelectric point (IEP) at pH 3.5, where the ice surface has no charge and therefore minimal adsorption of ions occurs. The full behaviour at the IEP, showing the equilibrium distances varying with the radius of the ice sphere for various background concentrations of salt ($NaNO_3$), is charted on Fig. 5 (using ice model 12, ϵ^{12}_{ice}). The behaviour of the equilibrium distance is similar to that found for the balance with the pure van der Waals interaction in Fig. 4. Buoyancy causes large ice particles ($a > 1$ cm) to make contact with the water-air interface, while an equilibrium distance as large as 2-7 nm is found for microscopic particles ($a < 10\mu$m). The microscopic equilibrium distance varies with salt concentration. At the lowest concentration (1 mM salt) the salt effect is negligible and the particle follows the pure van der Waals balance with an equilibrium distance around 2 nm. At high concentration (100 mM), salt effects are screened (the Debye length becomes shorter than the length scale of the van der Waals interaction), so again the behaviour follows the pure van der Waals case. In between, the salt effect induces repulsion due to the entropic contribution from the ion adsorption layer, $F_{\rm en}$ (Eq. 12). This salt-induced repulsion pushes the equilibrium distance out as far as 7 nm when the salt concentration is 4 mM.

For comparison, in Fig. 6 we show the equilibrium distances in neutral water (pH 7) at various salt concentrations. In this case the ice surface in 0.1 mM salt develops a relatively strong charge (−0.0024 C/m) and the repulsive impact of the ion adsorption layer is stronger, pushing the equilibrium distance out beyond 200 nm. But electrostatic screening at higher concentrations quenches the salt effect quite quickly. Already at 10 mM concentration, the system at pH 7 behaves equivalently to the pure van der Waals case with an equilibrium distance below 3 nm. We note that the transition point between macroscopic particles (contacting the water-air interface) and microscopic particles (repelled away from the water-air interface) occurs consistently at the same particle size, around 10–100 μm. Interestingly in pure water (with H^+ and OH^- at 10^{-7} M) the equilibrium distance becomes as large as one micron because of the low level of screening.

The limiting microscopic equilibrium distances (evaluated for ice particles with radius $a < 0.1\,\mu$m) are collected as a function of pH for various background salt concentrations in Fig. 7. At a given salt concentration salt-induced repulsion is found both above and below the isoelectric point. That is, the isoelectric point expresses as a relatively narrow peak, drawing microparticles closer towards the air-water interface where at other pH they would be pushed away. This isoelectric peak is seen clearly until salt concentrations rise to 50 mM, at which point the IEP simply provides a dip between low and high pH. We see that concentration affects the apparent position of the IEP, with the IEP peak moving from pH 3.5 in 1 mM salt to pH 4 in 100 mM salt. For reference, the surface charge and potential of the ice surface is shown in Supplementary Information.

The effect of concentration, as already seen, is to screen the impact of salt-induced repulsion. Above 10 mM concentrations

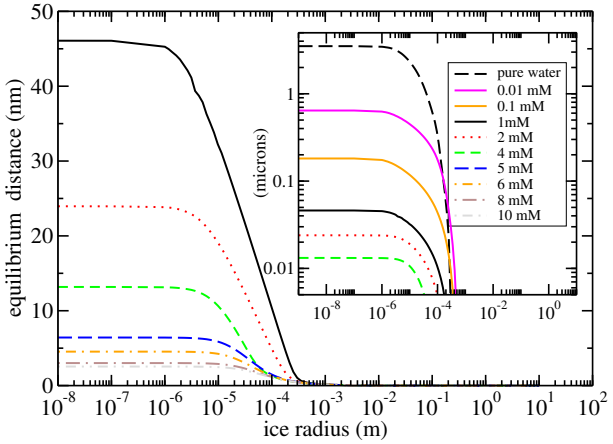

Fig. 6. (Color online) Equilibrium distance l_{eq} as a function of the sphere radii with the ice surface charged at pH 7. This is obtained as the distance with zero total force when adding net buoyancy force, Lifshitz force and forces due to salt ions (i.e. when $f_b + f_L(l_{eq}) + f_{\rm salt}(l_{eq}) = 0$). Curves are shown for a range of background $NaNO_3$ salt concentrations.

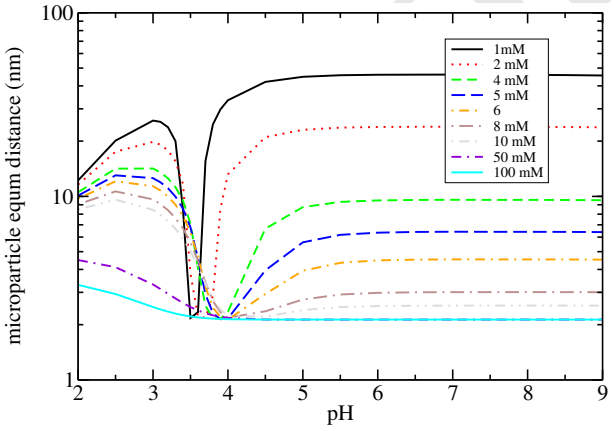

Fig. 7. (Color online) Microscopic equilibrium distance l_{eq} for spheres with radius $< 0.1\ \mu$m as a function of pH. This is obtained as the distance with zero total force when adding net buoyancy force, Lifshitz force and forces due to salt ions (i.e. when $f_b + f_L(l_{eq}) + f_{\rm salt}(l_{eq}) = 0$). Curves are shown for a range of background $NaNO_3$ salt concentrations.

(in the case of pH > IEP) and above 50 mM concentrations (pH < IEP), repulsion is dominated by the van der Waals interaction.

C. Consequences for Life. We observe in Fig. 6 that an exclusion zone free of small ice particles (less than 50 μm radius) is formed at the air-water interface. In low salinity water the exclusion zone may be several 100 nm thick, exceeding the size of biomolecules extruded by microorganism to form biofilms. Indeed, in pure water associated with freshly melting ice the exclusion zone is 1 μm, larger than the size of some bacteria. As larger ice particles penetrate the exclusion zone, the presence of smaller ice particles outside may induce an attractive depletion force helping any such biofilm or bacteria to adhere to large ice particles. This mechanism may contribute to the relatively greater number of bacteria observed at surfaces of arctic sea ice and glacial ice (23, 24). Exclusion of small ice particles may aid the adhesion of bacteria to large ice particles at the air-water interface.

4. Conclusions

We have recently investigated how thin films of ice can start to grow on a water-solid interface due to Lifshitz forces. (25) Here we have considered how ice growth occurs at a water surface. It is known that Lifshitz forces by themselves are not sufficient to cause an ice film to grow at a water-air surface (9). In the early stage of ice growth we suggest that Lifshitz-Derjaguin and double layer forces between ice structures and water surface cause small ice structures to accumulate in an equilibrium layer near a water surface. These aggregate to micrometer sized ice particles until gravity causes them to rise to the water-air surface. One would expect ice to cross the water surface when it comes very close. At this point there will be no Lifshitz repulsion and the ice will float with fraction above the water surface. As is well known in the equilibrium system for large particles, ice floats on water, possibly with a thin film of premelted water when ice is in contact with air (3).

We acknowledge support from the Research Council of Norway (Projects 221469, 250346 and 243642). We gratefully acknowledge support by the German Research Council (grant BU1803/3-1, S.Y.B. and J.F.) the Research Innovation Fund by the University of Freiburg (S.Y.B. and J.F.) and the Freiburg Institute for Advanced Studies (S.Y.B.). This work was supported by resources provided by The Pawsey Supercomputing Centre with funding from the Australian Government and the Government of Western Australia.

Supporting Information (SI). A brief description of the Casimir-Polder interaction in the limit of small sphere size ($a \ll z$). Figures of surface charges and potentials of ice in water at various pH and salt concentrations.

1. Weeks W (2010) *On sea ice.* (University of Alaska Press, Fairbanks).
2. Bartels-Rausch T, et al. (2012) Ice structures, patterns, and processes: A view across the icefields. *Rev. Mod. Phys.* 84(2):885–944.
3. Elbaum M, Schick M (1991) Application of the theory of dispersion forces to the surface melting of ice. *Phys. Rev. Lett.* 66(13):1713–1716.
4. Wilen LA, Wettlaufer JS, Elbaum M, Schick M (1995) Dispersion-force effects in interfacial premelting of ice. *Phys. Rev. B* 52(16):12426–12433.
5. Bar-Ziv R, Safran SA (1993) Surface melting of ice induced by hydrocarbon films. *Langmuir* 9(11):2786–2788.
6. Dash JG, Rempel AW, Wettlaufer JS (2006) The physics of premelted ice and its geophysical consequences. *Rev. Mod. Phys.* 78(3):695–741.
7. Thiyam P, et al. (2016) Effects of van der waals forces and salt ions on the growth of water films on ice and the detachment of co2 bubbles. *EPL (Europhysics Letters)* 113(4):43002.

8. Boström M, et al. (2016) The influence of lifshitz forces and gas on premelting of ice within porous materials. *EPL (Europhysics Letters)* 115(1):13001.
9. Elbaum M, Schick M (1991) On the failure of water to freeze from its surface. *Journal de Physique I* 1:1665–1668.
10. Derjaguin B, Landau L (1993) Theory of the stability of strongly charged lyophobic sols and of the adhesion of strongly charged particles in solutions of electrolytes. *Progress in Surface Science* 43(1):30 – 59.
11. Verwey EJW, Overbeek JTG (1948) *Theory of the Stability of Lyophobic Colloids*. (Elsevier).
12. Lide DR, ed. (2005) *CRC Handbook of Chemistry and Physics*. (CRC Press, Boca Raton, Florida), 86^{th} edition.
13. Danov KD, Kralchevsky PA, Boneva MP (2004) Electrodipping force acting on solid particles at a fluid interface. *Langmuir* 20(15):6139–6151. PMID: 15248696.
14. Cooray H, Cicuta P, Vella D (2017) Floating and sinking of a pair of spheres at a liquid–fluid interface. *Langmuir* 33(6):1427–1436. PMID: 28093906.
15. Dzyaloshinskii IE, Lifshitz EM, Pitaevskii LP (1961) General theory of van der waals' forces. *Soviet Physics Uspekhi* 4(2):153.
16. Davids PS, Intravaia F, Rosa FSS, Dalvit DAR (2010) Modal approach to casimir forces in periodic structures. *Phys. Rev. A* 82(6):062111.
17. Casimir HBG, Polder D (1948) The influence of retardation on the london-van der waals forces. *Phys. Rev.* 73(4):360–372.
18. Buhmann SY (2012) *Dispersion Forces I: Macroscopic Quantum Electrodynamics and Ground-State Casimir, Casimir–Polder and van der Waals Forces*, Springer Tracts in Modern Physics. (Springer, Heidelberg).
19. Fiedler J, Scheel S (2015) Casimir-polder potentials on extended molecules. *Annalen der Physik* 527(9-10):570–579.
20. Kallay N, Čop A, Chibowski E, Holysz L (2003) Reversible charging of the ice–water interface: Ii. estimation of equilibrium parameters. *Journal of Colloid and Interface Science* 259(1):89 – 96.
21. Parsons DF, Salis A (2015) The impact of the competitive adsorption of ions at surface sites on surface free energies and surface forces. *The Journal of Chemical Physics* 142(13):134707.
22. Logg A, Wells GN (2010) Dolfin: Automated finite element computing. *ACM Trans. Math. Softw.* 37(2):20:1–20:28.
23. Junge K, Eicken H, Deming JW (2004) Bacterial activity at -2 to -20° c in arctic wintertime sea ice. *Applied and Environmental Microbiology* 70(1):550–557.
24. Mader HM, Pettitt ME, Wadham JL, Wolff EW, Parkes RJ (2006) Subsurface ice as a microbial habitat. *Geology* 34(3):169.
25. Boström M, et al. (2017) Lifshitz interaction can promote ice growth at water-silica interfaces. *Phys. Rev. B* 95(15):155422.